CALIBRATION OF PRESSURE SENSORS

MARTIN VARGA, TATIANA KELEMENOVA, MICHAL KELEMEN, IVAN VIRGALA, LUBICA MIKOVA, ERIK PRADA, PETER MARCINKO, MAREK SUKOP, DOMINIK NOVOTNY

Technical University of Kosice, Faculty of Mechanical Engineering, Kosice, Slovakia

DOI: 10.17973/MMSJ.2023_10_2023075

michal.kelemen@tuke.sk

The aim of the work is to calibrate the liquid pressure sensor, for which the manufacturer provides only basic data. However, there is a lack of data on other properties of the sensor needed before its use. The properties of the sensor must therefore be verified and identified. The article presents a methodology for quick identification of basic sensor parameters. These activities are also necessary during the input inspection of the sensors for their integration into the selected application.

KEYWORDS

pressure sensor, gauges, uncertainty, calibrator

1 INTRODUCTION

There is a whole range of sensors on the market, and before their implementation, it is necessary to verify their application possibilities and their behavior in the given application. It may happen that, despite the declared properties, the sensor behaves differently and this may have various reasons. It can be non-standard situations, use outside the prescribed conditions or it can be a sensor failure due to bad handling of this sensor. There are also situations when there is not enough information for the sensor, so it is necessary to find it out and verify its application possibilities.

The aim of the work is to perform the calibration of the fluid pressure sensor, for which the manufacturer provides only basic data on the range and size of the output voltage and the maximum measurement error. However, there is a lack of data on other properties of the sensor such as hysteresis, dead zone, linearity and calibration characteristic for the conversion of electrical voltage to pressure value. Therefore, it is necessary to completely verify the sensor and identify its unknown properties [EA-4/02 1999, JCGM 100 2008, JCGM 104 2009, Hortobagyi 2021, Kelemen 2021, Kelemenova 2021a, Kelemenova 2021b, Mikova 2022].

2 VERIFIED SENSOR AND METHODOLOGY OF VERIFICATION AND IDENTIFICATION OF ITS PROPERTIES

A pressure sensor (Fig. 1) from an unknown manufacturer is available, for which the supplier provided only basic information. The sensor is intended for measuring the pressure of liquids or gases. It is a piezoresistive membrane pressure sensor in a stainless steel case and is also suitable for use in industrial conditions and in automotive applications. It can be used to measure oil pressure, fuel pressure, brake system pressure, pneumatic system pressure and other similar applications.

The measured pressure range is 200 kPa (30 psi; 2 bar). The output of this sensor is an electrical voltage in the range of 0.5 to 4.5 V, which should be linear and it is not indicated whether hysteresis occurs. The maximum sensor overload is 400 kPa. The accuracy of the sensor is defined as 1% of the nominal pressure value. The working temperature range is -20°C to 100°C. The connecting pressure terminal is a threaded end with a diameter of 1/4"NPT. The sensor has IP protection at the IP65 level, which according to the IEC standard means that it is dustproof and waterproof with resistance against intense splashing water.

Figure 1. Verified pressure sensor

The tested sensor lacks information about its calibration characteristic, which will allow recalculation of the output voltage into information about the measured pressure, and it will be necessary to check the linearity of the sensor. It is not clear whether the output voltage also shows hysteresis and whether the sensor has a dead zone, i.e. an area in which it has reduced sensitivity to pressure changes [Trojanova 2021]. It will be necessary to determine both measurement errors and measurement uncertainty in the proposed measurement chain.

Handheld Pneumatic Pressure Test Pump (Fig. 2) will be used to test this pressure sensor. The Additel 914 pneumatic pressure test pump was selected (Fig. 2).

Figure 2. Handheld Pneumatic Pressure Test Pump

It is a hand operated pressure pump designed to generate pressure from 95% vacuum to 375psi (25bar). A high-quality screw press is designed for fine pressure adjustment, with an adjustment resolution up to 10 Pa (0.1 mbar). A specially designed shut-off valve makes the pressure as stable as possible during calibration. A built-in gas-liquid isolator protects the pump from moisture and dirt to reduce the need for maintenance [Kuznetsov 2020]. Two hand-tight quick connectors installed on the pump allow easy connecting and disconnecting to the test pump without the need for PTFE tape or wrenches.

The Handheld Pneumatic Pressure Test Pump is essentially just a pressure generator and allows the connection of two pressure measuring devices, one of which should be a reference pressure gauge and the other should be a verified pressure sensor or other pressure gauge.

Digital pressure gauge Additel 681 (Fig. 3) was chosen as a reference pressure gauge. It is a microprocessor pressure reference gauge with a dual analog and digital display for displaying the measured value. The measurement range is 2 MPa and the maximum permissible error (MPE) is set by the manufacturer at +-0.025% of the nominal value. This reference gauge enables data processing and displays the maximum and minimum value in various selectable pressure units.

The handheld pneumatic pressure test pump will have this reference pressure gauge and the tested pressure sensor connected (Fig. 4).

Figure 3. Digital Pressure Gauge Additel 681

Figure 4. Handheld Pneumatic Pressure Test Pump

The testing methodology consists in gradually slowly increasing the pressure to the pressure sensor and the reference pressure gauge, and then gradually the pressure is slowly released. The values in the process of increasing and decreasing the pressure are recorded and evaluated. The process is repeated three times to determine the repeatability of the measurement with the tested sensor.

3 ASSESSMENT OF SELECTED METROLOGICAL CHARACTERISTICS

Data from the measurement process were displayed as a transformation characteristic, where the value of the reference pressure was set and the output voltage values of the sensor were monitored. The calibration characteristic is created by flipping the axis of the graph, and the created mathematical model can then be used to convert the electrical voltage of the sensor to the measured pressure. In this way, three measurement cycles were realized, while in each cycle the pressure was gradually increased and then the pressure was gradually decreased (Fig. 5, 6, 7).

Assessment of the linearity of the graphic course of the measured values of the transformation characteristics is possible in several ways. A good indicator is the coefficient of determination R^2, which is determined in the regression of experimental data using a linear model:

$$R^2 = 1 - \frac{SS_{REGRESION}}{SS_{TOTAL}} = 1 - \frac{\sum_{i=1}^{n}(y_i - \hat{y}_i)^2}{\sum_{i=1}^{n}(y_i - \bar{y})^2}. \quad (1)$$

Where

$SS_{REGRESION}$ is sum squared regression error also called as residual sum of squares,

SS_{TOTAL} is sum squared total error is proportional to variance of data.

Coefficient of determination (pronounced "R squared") is the proportion of the variation in the dependent variable that is predictable from the independent variable. R^2 is a measure of the correctness of fit of a model. In regression, the R^2 coefficient of determination is a statistical measure of how well the regression predictions approximate the real data points. A value R^2 of 1 indicates that the regression predictions perfectly fit the data. Normally, R^2 is in the interval from 0 to 1, but Values of R^2 outside the range 0 to 1 occur when the model fits the data worse than the worst possible least-squares predictor (equivalent to a horizontal hyperplane at a height equal to the mean of the observed data). This occurs when a wrong model was chosen. The coefficients of determination obtained from the data analysis (Tab. 1) show that the values for all experimental runs are close to 1 and this indicates that the experimental data are in excellent agreement with the linear model.

Table 1. Coefficient of determination

Mode	Coefficient of determination for measurements		
	Measurement 1	Measurement 2	Measurement 3
Pressure increasing	0.9999833066	0.999997696	0.999997898
Pressure reduction	0.999955194	0.999993987	0.999914838

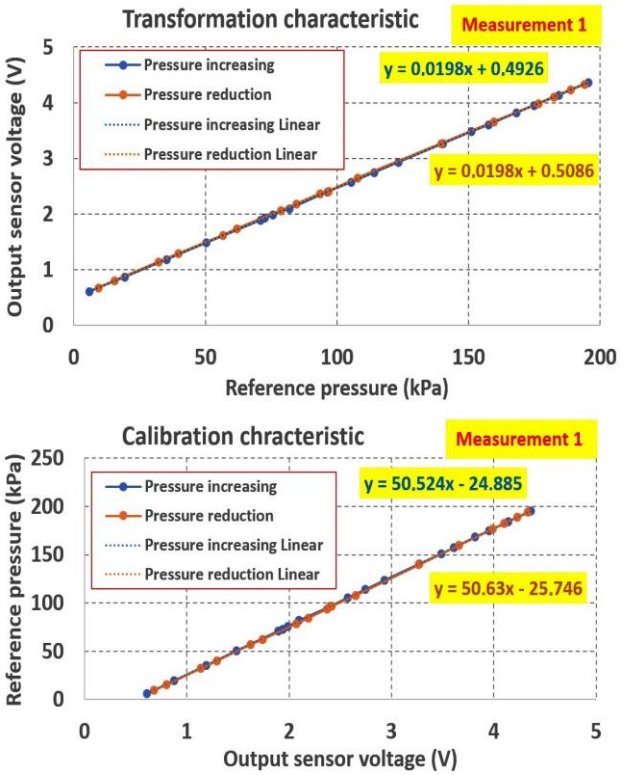

Figure 5. Transformation and calibration characteristics of the measured values for the 1st measurement cycle with continuous pressure increase and decrease

Maximum deviation from linearity is often used to express linearity and is expressed as the difference between the output experimentally determined quantity and the fitted value determined from the regression model:

$$D_{LIN} = MAX\left|y_i - \hat{y}_i\right|. \quad (2)$$

Where

y_i is experimental value,

$\hat{y}_i$ is residual fitted value.

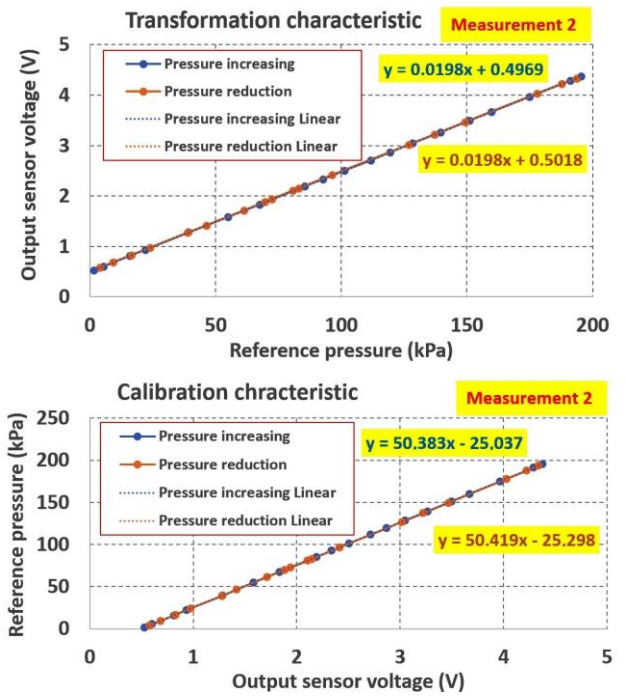

Figure 6. Transformation and calibration characteristics of the measured values for the 2nd measurement cycle with continuous pressure increase and decrease

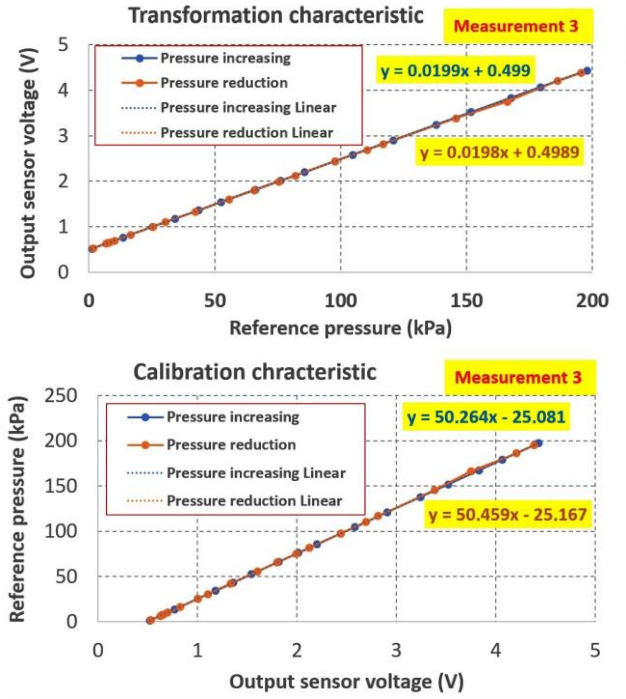

Figure 7. Transformation and calibration characteristics of the measured values for the 3rd measurement cycle with continuous pressure increase and decrease

Standard error from linearity provides the typical deviation from the linear behaviour of a fitted line prediction equation:

$$SE_{LIN} = \sqrt{\frac{1}{n-2}\sum_{i=1}^{n}\left(y_i - \hat{y}_i\right)^2}\ . \qquad (3)$$

Both methods [Hogan 2019] ("Maximum deviation from linearity" and "Standard error from linearity") evaluate the deviation from linearity. The difference between these two methods is first method evaluates the worst-case scenario and the other second method evaluates the most likely or most probable scenario. Both methods are summarized in Tab. 2.

Results evaluates by first method (Maximum deviation from linearity) are below the threshold of 0.62% in percentage terms.

Table 2. Maximum deviation from linearity and Standard error from linearity

Linearity evaluation	Maximum deviation from linearity and Standard error from linearity		
	Measurement 1	Measurement 2	Measurement 3
Maximum deviation from linearity (V); (%) Pressure increasing	0.010499 0.54%	0.006039 0.47%	0.002922 0.08%
Maximum deviation from linearity (V); (%) Pressure reduction	0.016315 0.62%	0.006686 0.52%	0.017279 0.41%
Standard error from linearity (V) Pressure increasing	0.004745	0.001944	0.001837
Standard error from linearity (V) Pressure reduction	0.008510	0.003097	0.011893

Another phenomenon that needs to be known about the sensor under study is hysteresis. On the graphic course (Fig. 8) it can be seen that the input value X_H corresponds to two values of the output quantity Y_{H_LOAD} and $Y_{H\_RELEASE}$. This ambiguity is a big problem from the point of view of measurement, and when processing such a signal, we cannot clearly assign the correct corresponding value of the output quantity. And the same phenomenon occurs with the calibration characteristic.

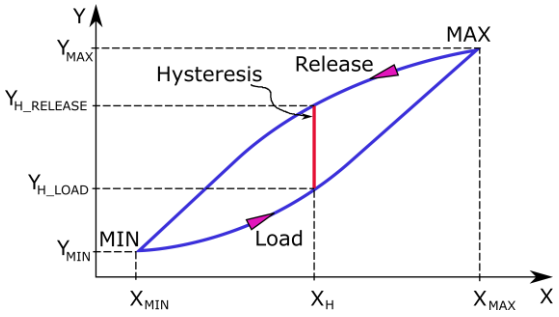

Figure 8. Determination of sensor hysteresis

The hysteresis of the sensor is the absolute value (Fig. 8) of the largest difference between the values of the output signal corresponding to the same value of the input signal. Hysteresis is an error of the sensor, which is caused by the fact that the transformation characteristics differ depending on the direction in which the change of the stimulus occurs: whether it is an increase in its values or a decrease in them. This value of hysteresis can then be determined according to the relationship:

$$HS = \left|\frac{Y_{H\_LOAD} - Y_{H\_RELEASE}}{Y_{MAX} - Y_{MIN}}\right| \cdot 100\,. \qquad (4)$$

It is evident from the transformation characteristics that the hysteresis is minimal, and the calculated values are very small (Tab. 3) and thus it is possible to conclude that the sensor shows only minimal hysteresis. Hysteresis can only be seen on

the graph after increasing the course of the transformation characteristic (Fig. 9).

Table 3. Hysteresis of sensor

Linearity evaluation	Measurement		
	Measurement 1	Measurement 2	Measurement 3
Hysteresis (%)	0.43%	0.12%	0.003%

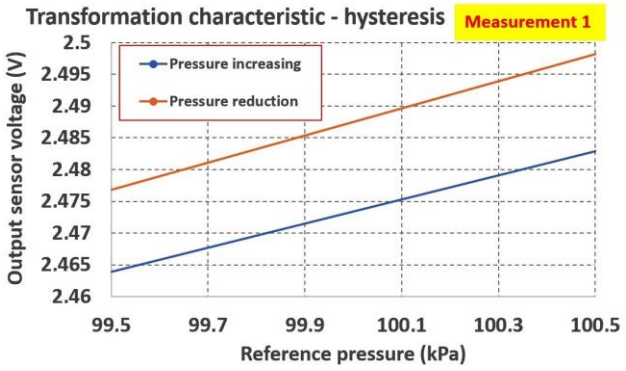

Figure 9. Sensor hysteresis

The zone of insensitivity of the sensor – also called as "dead zone" is the maximum range of values of the input signal, at which there is no noticeable change in the output data from the steady value, in the case of the tested sensor, this means that there is still no response at the sensor output even if there is a change in pressure. This phenomenon occurs mainly at low pressure values and can be checked on the enlarged view of the transformation characteristic (Fig. 10), from which it can be seen that this phenomenon does not occur or was not detected during testing.

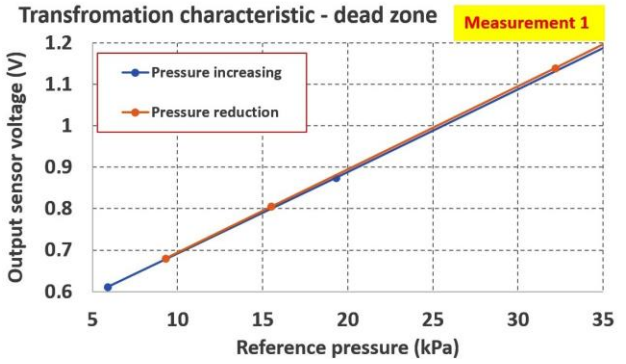

Figure 10. Dead zone of sensor

The repeatability of the sensor is the ability of the sensor to detect values very close to the same value of the quantity during repeated measurements under the same measurement conditions. This property of the sensor can be verified by displaying all measurements in one graph (Fig. 11).

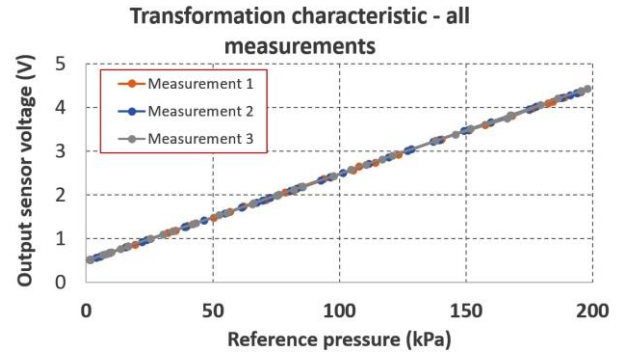

Figure 11. Repeatability of sensor

The results of all measurements completely overlap, so it can be concluded that the sensor has excellent repeatability.

Mathematical regression models were implemented on all transformation characteristics, which were created by approximation by linear dependence. Thanks to the excellent repeatability of the sensor, these mathematical models can be replaced by one common mathematical model in a linear form. The coefficients of this mathematical model can be determined as the arithmetic mean of the corresponding coefficients from all partial mathematical models. And so in the graph with all measurements (Fig. 12) it is possible to display the obtained overall mathematical model of the transformation characteristics of the investigated sensor:

$$V_S = 0.01982 \cdot p + 0.4996 . \quad (5)$$

Where p is measured pressure.

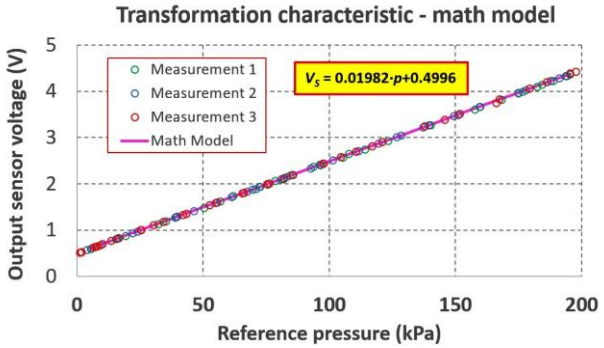

Figure 12. Mathematical model of transformation characteristics of the sensor

Several additional information can be obtained from the obtained mathematical model.

The sensitivity of the sensor is the ratio of the change in the value of the output signal dy to the change in the measured value dx, and the coefficient a is the sensitivity of the tested sensor:

$$k_C = \lim_{\Delta x \to 0} \frac{\Delta y}{\Delta x} = \frac{dy}{dx} = 0.01982 \text{ V/kPa} . \quad (6)$$

The sensitivity is therefore the ratio of the difference in the values of the output signals Δy to the difference in the corresponding values of the input stimuli Δx and in this case it means that the output voltage of the sensor increases by 0.01982 V when the pressure increases by 1 kPa.

Zero drift or bias describes the effect where the zero reading of an instrument is modified by a change in ambient conditions. This causes a constant error that exists over the full range of measurement of the instrument. This sensor has a zero drift of 0.4996 V, which is actually the coefficient b from the obtained overall mathematical model ($y = ax + b$). This means that at a pressure of 0 kPa, the output voltage value of the sensor will be exactly equal to the zero drift value. Zero drift is not a problem, because it can be read as a result, since its value is constant in the entire measurement range of the sensor. The existence of zero drift also has an advantage in the operation of the sensor, because the zero value of the electric voltage will mean a fault on the sensor, which will be easily diagnosed in this way.

4 MATH MODEL OF MEASUREMENT AND UNCERTAINTY OF MEASUREMENT

The calibration characteristics of individual measurements were fitted with a linear model and described by a mathematical model using regression analysis. From these three measurements, there are three mathematical models, from

which the resulting mathematical model is created in such a way that arithmetic averages were created from the individual coefficients of the mathematical models, and these new constants form the overall mathematical model of the calibration characteristic (Fig. 13), or otherwise also called the mathematical model of the measurement:

$$p = 50.4465 \cdot V_S - 25.2023. \quad (7)$$

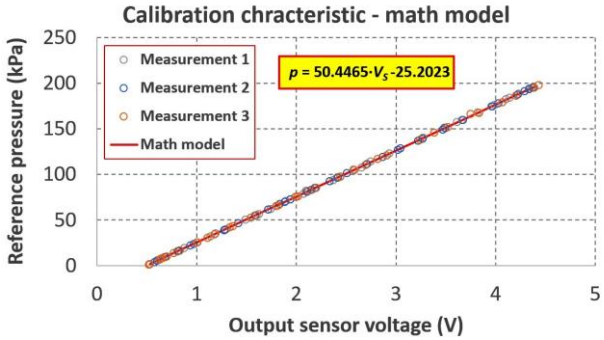

Figure 13. Mathematical model of calibration characteristics of the sensor

The obtained mathematical model from the calibration characteristic enables the conversion of the measured values of the output electric voltage of the pressure sensor to the values of the measured pressure, and this conversion can be realized by a microcontroller or a programmable logic controller or another computing system.

According to this measurement model, the mentioned pressure measurement using the assessed sensor is an indirect measurement, because the resulting value must be obtained by calculation from other measured or calculated values, and thus measurement uncertainties must be analyzed according to the standards.

The mathematical model of the calibration characteristic enables the calculation of the desired values of the measured pressure, but in order for the result to be complete, it is necessary that the uncertainties of the pressure values are also determined. The mathematical model of the calibration characteristic ($y = ax + b$) contains, in addition to the values of the output electric voltage (at position x in math model), also the values of the coefficients (a, b), which are determined from the experimental values of pressure (at position y in math model) and electric voltage, which have their measurement uncertainties. So these coefficients (a, b) will also have their determination uncertainties:

$$u^2_{(a)} = \frac{n}{n\sum_{i=1}^{n} x_i^2 - \left(\sum_{i=1}^{n} x_i\right)^2} \cdot \sigma^2. \quad (8)$$

$$u^2_{(b)} = \frac{\sum_{i=1}^{n} x_i^2}{n\sum_{i=1}^{n} x_i^2 - \left(\sum_{i=1}^{n} x_i\right)^2} \cdot \sigma^2. \quad (9)$$

The covariance between these coefficients (a, b) can also significantly affect the resulting uncertainty, so it is necessary to determine it:

$$u_{a,b} = \mathrm{cov}(a,b) = \frac{-\sum_{i=1}^{n} x_i}{n\sum_{i=1}^{n} x_i^2 - \left(\sum_{i=1}^{n} x_i\right)^2} \cdot \sigma^2 \cdot \quad (10)$$

Where σ is standard deviation of distance (y_i) is possible to estimate with residual variance (also mentioned as Standard error from linearity):

$$\sigma^2_{MSE} = \frac{1}{n-2}\sum_{i=1}^{n}\left[y_i - (a \cdot x_i + b)\right]^2. \quad (11)$$

For our linear model of the calibration characteristic, it is then possible to determine the standard uncertainty of the measured pressure from the given values:

$$u_y = \sqrt{(u_b^2 + x^2 \cdot u_a^2) + a^2 \cdot u_x^2 + 2\left(x \cdot u_{a,b}\right)}. \quad (12)$$

According to this equation, standard measurement uncertainties are calculated for individual pressure values (Fig. 14).

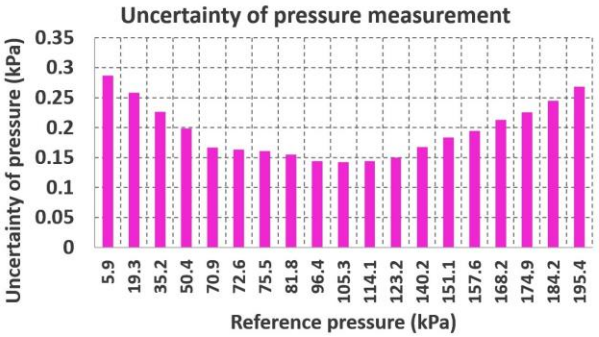

Figure 14. Standard uncertainty of measure pressure

The calculation of the standard uncertainties of the pressure measurement was carried out from the data from measurement 1, where the linearity deviation was the largest (worst case). From the displayed values of the calculated standard uncertainties, it is obvious that they are all smaller than 0.3 kPa, which represents 0.2% of the nominal value of the largest measured pressure.

The resulting uncertainties also include the uncertainties of the standard, calibrator and multimeter, which were used to measure the output voltage of the sensor. By using a better measuring device for electrical voltage, it is possible to achieve even more favorable values of uncertainties.

With some sensors, there is a tendency for the output value of the sensor to drift when used for a long time. This phenomenon has been observed with some types of sensors. The temporal stability of the sensor signal seems to be important in order not to increase the measurement error of the sensor. In the next step, the stability of the sensor's output signal will be monitored. A handheld pneumatic pressure test pump is used and with its help a pressure is created at the maximum value of the sensor range (200 kPa), which is kept at a constant value for 2 hours and the stability of the output signal is monitored every minute (Fig. 15). During this time, the pressure was monitored using the sensor and at the same time the pressure on the reference standard gauge, so that pressure instability in the handheld pneumatic pressure test pump could also be monitored [Murcinkova 2013]. The measured data indicate a small pressure instability (Fig. 15) which was detected by the reference standard gauge and this graph of pressure instability was partially followed by the pressure graph measured by the sensor (Fig. 15). In order to determine the instability of the sensor signal itself, it is then possible to determine the difference of these values (of the sensor and the reference standard gauge) in order to rule out the influence of the instability of the test pump [Bozek 2021]. From this deviation form, only the instability of the output signal of the sensor (Fig. 16) can be seen, which is in the range of less than 1 kPa, which represents 0.5% of the nominal value.

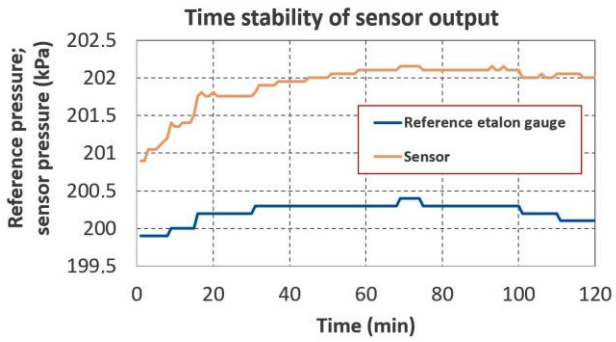

Figure 15. Time stability of sensor output signal

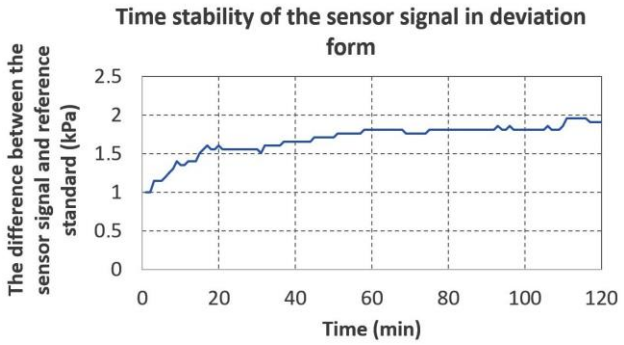

Figure 16. Time stability of sensor signal expressed as the difference between the value of the sensor signal and the value of the reference standard

5 CONCLUSIONS

In this work, the metrological properties of the investigated pressure sensor were verified and unknown properties were also identified, which were not mentioned by the manufacturer or supplier of the sensor. This recognition of the sensor's property is very important for the application of this sensor in a specific system.

Three independent measurement cycles were carried out under the same measurement conditions, and transformation and calibration characteristics were created from them, which were approximated by a linear model, and mathematical models of these characteristics were created.

The linearity of the transformation characteristics was investigated by three indicators. The first indicator of linearity is the coefficient of determination R2, which is determined in the regression of experimental data using a linear model, and its value expresses the degree of agreement with the linear model. The values of the coefficients of determination for the predicates of the three waveforms are very close to zero, so the transformation characteristics are in very good agreement with the linear model. Another indicator is the maximum deviation from linearity, which is a maximum of 0.62%. The third indicator is the standard error from linearity, which is a maximum of 11 mV for all transformation characteristics. The linearity of the transformation characteristics is very well described by a linear model with minimal linearity deviation.

The hysteresis of the transformation characteristic is an unfavorable phenomenon that negatively affects the application of the sensor, and its value was determined with a maximum size of 0.43%, which means that the sensor shows only minimal or almost no hysteresis.

The dead zone of the sensor was investigated on the transformation characteristics and no dead zone was found that would negatively affect the application of the sensor.

The agreement between the individual measurement cycles confirmed the excellent repeatability of the assessed pressure sensor.

From the resulting mathematical model, the sensitivity was determined to be 0.01982 V/kPa and the zero drift is 0.4996 V.

The resulting calibration characteristic of the sensor is approximated by a mathematical measurement model, which can be used to convert the sensor's output electrical voltage to the measured pressure value. Based on this mathematical model of the calibration characteristic, measurement uncertainties were determined for the pressure values measured by the tested sensor, which are a maximum of 0.3 kPa, which represents a maximum of 0.2% of the nominal value of the measured pressure.

The temporal stability of the sensor signal was monitored at the maximum pressure value maintained for 2 hours. The instability of the signal was a maximum of 1 kPa.

Although it is a cheap sensor, its features are excellent compared to the best sensors of this type available on the market.

The benefit of this article is the sensor testing methodology, which can be used as an input check when receiving the ordered sensors. Checking the metrological properties of sensors is a key activity, because the overall functionality of products and devices often depends on the qualitative properties of sensors [Blatnicky 2020, Hroncova 2022a, Hroncova 2022b, Klarak 2021, Koniar 2014, Lestach 2022, Mascenik 2014 and 2021, Nikitin 2020, Peterka 2020, Pivarciova 2021, Sincak 2021, Suder 2021, Saga 2018, Saga 2020, Virgala 2022, Zelnik 2021].

ACKNOWLEDGMENTS

The authors would like to thank the Slovak Grant Agency - project KEGA 027TUKE-4/2022, project KEGA 054TUKE-4/2022 and project KEGA 016TUKE-4/2021.

This publication was created thanks to support under the Operational programme Integrated Infrastructure for the project Center for the Development of Textile Intelligence and Antimicrobial Technologies co-financed by European Regional Development Fund. ITMS2014+ 313011AVF5 Center for the Development of Textile Intelligence and Antimicrobial Technologies.

REFERENCES

[Blatnicky 2020] Blatnicky M. et al. Design of a Mechanical Part of an Automated Platform for Oblique Manipulation. Applied Sciences, 2020, Vol. 10, No. 23, Art. No. 8467. DOI 10.3390/app10238467.

[Bozek 2021] Bozek, P., Nikitin, Y., Krenicky, T. The Basics Characteristics of Elements Reliability. In: Diagnostics of Mechatronic Systems. Series: Studies in Systems, Decision and Control, 2021, Vol. 345, pp. 1-15. ISBN 978-3-030-67055-9.

[EA-4/02 1999] Expression of the Uncertainty of Measurement in Calibration. European co-operation Accreditation Publication Reference, 1999.

[Hogan 2019] Hogan, R. How to Calculate Linearity Uncertainty. Available online. Cited 2019-06-18. Published 2019-4-8. https://www.isobudgets.com/how-to-calculate-linearity-uncertainty/.

[Hortobagyi 2021] Hortobagyi, A. et al. Holographic Interferometry for Measuring the Effect of Thermal Modification on Wood Thermal Properties. Applied

Sciences, Vol.11, No. 6, 2021, pp. 1-11. DOI: 10.3390/app11062516.

[Hroncova 2022a] Hroncova, D. et al. Robot Trajectory Planning. MM Science Journal, 2022, pp. 6098-6108. DOI: 10.17973/MMSJ.2022_11_2022093.

[Hroncova 2022b] Hroncova, D. et al. Forward and inverse robot model kinematics and trajectory planning. In: 20th Int. Conf. on Mechatronics - Mechatronika (ME); Pilsen, Czech Republic, 2022, pp. 1-9. DOI: 10.1109/ME54704.2022.9983355.

[JCGM 100 2008] JCGM 100 – Evaluation of measurement data – Guide to the expression of uncertainty in measurement (ISO/IEC Guide 98-3). 1st edition, 2008. Available online: http://www.iso.org/sites/JCGM/GUM-JCGM100.htm.

[JCGM 104 2009] Evaluation of measurement data – An introduction to the "Guide to the expression of uncertainty in measurement" (ISO/IEC Guide 98-1). 1st edition, 2009. Available online: http://www.bipm.org/en/publications/guides/gum_print.html.

[Kelemen 2021] Kelemen, M. et al. Head on Hall Effect Sensor Arrangement for Displacement Measurement. MM Science Journal, 2021, pp. 4757-4763. DOI: 10.17973/MMSJ.2021_10_2021026.

[Kelemenova 2021a] Kelemenova, T. et al. Verification of Force Transducer for Direct and Indirect Measurements. MM Science Journal, 2021, Vol. October, pp. 4736-4742. DOI: 10.17973/MMSJ.2021_10_2021021.

[Kelemenova 2021b] Kelemenova, T. et al. Verification of the Torque Gauges. MM Science Journal, 2022, Vol. March, pp. 5533-5538. DOI: 10.17973/MMSJ.2022_03_2022014.

[Klarak 2021] Klarak, J. et al. Analysis of Laser Sensors and Camera Vision in the Shoe Position Inspection System. Sensors, 2021, Vol. 21, No. 22, pp. 1-20. DOI: 10.3390/s21227531.

[Koniar 2014] Koniar, D. et al. Virtual Instrumentation for Visual Inspection in Mechatronic Applications. Procedia Engineering, Vol. 96, pp. 227-234. DOI: 10.1016/j.proeng.2014.12.148.

[Kuznetsov 2020] Kuznetsov, E., Nahornyi, V., Krenicky, T. Gas Flow Simulation in The Working Gap of Impulse Gas-barrier Face Seal. Management Systems in Production Engineering, 2020, Vol. 28, No. 4, pp. 298-303.

[Lestach 2022] Lestach, L. et al. Two-legged Robot Concepts. MM Science Journal, 2022, Vol. October, pp. 5812-5818. DOI: 10.17973/MMSJ.2022_10_2022091.

[Mascenik 2014] Mascenik, J., Pavlenko, S. Determining the exact value of the shape deviations of the experimental measurements. Applied Mechanics and Materials, 2014, Vol. 624, pp. 339-343.

[Mascenik 2021] Mascenik, J. and Pavlenko, S. Controlled testing of belt transmissions at different loads. MM Science Journal, 2021, Vol. December, pp. 5497-5501. DOI: 10.17973/MMSJ.2021_12_2021045.

[Nikitin 2020] Nikitin, Y.R. et al. Logical–Linguistic Model of Diagnostics of Electric Drives with Sensors Support. Sensors, 2020, Vol. 20, Iss. 16, pp. 1-19.

[Mikova 2022] Mikova, L. et al. Upgrade of Biaxial Mechatronic Testing Machine for Cruciform Specimens and Verification by FEM Analysis. Machines, 2022, Vol. 10, No. 10, pp. 1-29. DOI: https://doi.org/10.3390/machines10100916.

[Murcinkova 2013] Murcinkova, Z., Krenicky, T. Implementation of virtual instrumentation for multiparametric technical system monitoring. In: SGEM 2013: 13th Int. Multidisciplinary Sci. Geoconf., Vol. 1; 16-22 June, 2013, Albena, Bulgaria. Sofia: STEF92 Technology, 2013, pp. 139-144. ISBN 978-954-91818-9-0.

[Peterka 2020] Peterka, J. et al. Diagnostics of Automated Technological Devices. MM Science Journal, 2020, Vol. October, pp. 4027-4034. DOI: 10.17973/MMSJ.2020_10_2020051.

[Pivarciova 2021] Pivarciova, E. et al. Interferometric Measurement of Heat Transfer above New Generation Foam Concrete. Measurement Science Review, 2019, Vol. 19, No. 4, pp. 153-160. DOI: 10.2478/msr-2019-0021.

[Saga 2018] Saga, M. et al. Effective algorithm for structural optimization subjected to fatigue damage and random excitation. Scientific J. of Silesian Univ. of Technology-Series Transport, 2018, Vol. 99. DOI: 10.20858/sjsutst.2018.99.14.

[Saga 2020] Saga, M. et al. Case study: Performance analysis and development of robotized screwing application with integrated vision sensing system for automotive industry. Int. J. of Adv. Robotic Systems, 2020, Vol. 17, No. 3, 172988142092399. https://doi.org/10.1177/1729881420923997.

[Sincak 2021] Sincak, P.J. et al. Chimney Sweeping Robot Based on a Pneumatic Actuator. Applied Sciences, 2021, Vol. 11, No. 11, 4872. https://doi.org/10.3390/app11114872.

[Suder 2021] Suder, J. et al. Experimental Analysis of Temperature Resistance of 3D Printed PLA Components. MM Science Journal, 2021, Vol. March, pp. 4322-4327. DOI: 10.17973/MMSJ.2021_03_2021004.

[Trojanova 2021] Trojanova, M., Cakurda, T., Hosovsky, A., Krenicky, T. Estimation of Grey-Box Dynamic Model of 2-DOF Pneumatic Actuator Robotic Arm Using Gravity Tests. Applied Sciences, 2021, Vol. 11, No. 10, Art. No. 4490.

[Virgala 2022] Virgala, I. et al. Biped Robot with unconventional kinematics. MM Science Journal, 2020, Vol. October, pp. 5819-5824. DOI: 10.17973/MMSJ.2022_10_2022092.

[Zelnik 2021] Zelnik, R. et al. Research and Diagnostics for the Laboratory of Pressure Resistant Sensors. MM Science Journal, 2021, Vol. October, pp. 4853-4856. DOI: 10.17973/MMSJ.2021_10_2021041.

CONTACTS:

Michal Kelemen, prof. Ing. PhD.
Technical University of Kosice, Faculty of Mechanical Engineering
Institute of Automation, Mechatronics, Robotics and Production Techniques
Letna 9, 04200 Kosice, Slovak Republic
michal.kelemen@tuke.sk